Practical Advanced Analysis for Semi-rigid Frame Design

SEUNG-EOCK KIM and WAI-FAH CHEN

ABSTRACT

This paper presents three practical advanced analysis procedures for a two-dimensional semi-rigid steel frame design. Herein, the nonlinear behavior of beam-to-column connections is discussed, and practical modeling of these connections is introduced. The proposed methods can predict accurately the combined nonlinear effects of connection, geometry, and material on the behavior and strength of semi-rigid frames. The strengths predicted by these methods are compared well with those available experiments. Analysis and design procedures using the proposed methods are described in detail, and a case study is also given. The proposed procedures can be used for the LRFD design without tedious separate member capacity checks, including the calculations of K-factor. The procedures are suitable for adoption in practice.

INTRODUCTION

Conventional analysis and design of steel framed structures are usually carried out under the assumption that the beam-to-column connections are either fully rigid or ideally pinned. However, most connections used in current practice are semi-rigid type whose behavior lies between these two extreme cases. In the AISC-LRFD Specification,[1] two types of constructions are designated: Type FR (fully restrained) construction; and Type PR (partially restrained) construction. The LRFD Specification permits the evaluation of the flexibility of connections by rational means when the flexibility of connections is accounted for in the analysis and design of frames.

The semi-rigid connections influence the moment distribution in beams and columns as well as the drift and P-Δ effect of the frame. One way to account for all these effects in semi-rigid frame design is through the use of a direct second-order inelastic frame analysis known as "Advanced Analysis." Advanced analysis indicates a method that can sufficiently capture the limit state strength and stability of a structural system and its individual members so that separate member capacity checks are not required. Since the power of personal computers and engineering workstations is rapidly increasing, it is feasible to employ advanced analysis techniques directly in engineering design office. Herein, we shall develop a practical advanced analysis/design method for planar semi-rigid frames without the use of K-factor.

Since the study is limited to two-dimensional steel frames, the spatial behavior of frames is not considered here and lateral torsional buckling of members is assumed to be prevented by adequate lateral braces. This study covers both braced as well as unbraced semi-rigid frames. A compact W-section is assumed so that the section can develop full plastic moment capacity without local buckling.

Seung-Eock Kim is graduate research assistant, structures area of school of civil engineering, Purdue University, West Lafayette, IN.

Wai-Fah Chen is professor and head of structures area of school of civil engineering, Purdue University, West Lafayette, IN.

BEHAVIOR OF SEMI-RIGID FRAMES

The important attributes which affect the behavior of semi-rigid steel framed structures may be grouped into three categories: connection, geometric, and material nonlinearities. The connection nonlinearity indicates the nonlinear moment-rotation relationship of semi-rigid connections. The geometric nonlinearity includes second-order effects associated with the P-δ and P-Δ effects and geometric imperfections. The material nonlinearity includes gradual yielding associated with the influence of residual stresses on flexure behavior.

Nonlinear Behavior of Connections

The forces transmitted through beam-column connections consist of axial force, shearing force, bending moment, and torsion. The effect of axial force and shearing force is negligible since their deformations are small compared with the rotational deformation of connections, and torsion is also neglected since the present study is limited to planar frames. The deformation behavior of a connection may be customarily described by moment-rotation relationship, and its typical behavior is nonlinear. The schematic moment-rotation curves of commonly used semi-rigid connections are shown in Figure 1. It may be observed that a relatively flexible connection has a smaller ultimate moment capacity and a larger rotation, and vice versa. Herein, Kishi-Chen power model shall be adopted to describe the moment-rotation relationship of semi-rigid connections.[2]

If the direction of incremental moment applied to a connection is reversed, the connection will unload with the initial slope of the moment-rotation curve. This loading and unloading behaviors of connections can be adequately accounted for by the use of tangent stiffness and initial stiffness, respectively.[3] Herein, these stiffnesses shall be obtained by simply differentiating Kishi-Chen power model equation.

Geometric Nonlinearity

The bending moments in a beam-column consist of two types: primary bending moment; and secondary bending moment. Primary bending moments are caused by applied end moments and/or transverse loads on members. Secondary bending moments are from axial compressive force acting through the lateral displacements of a member. The secondary bending moments include the P-δ and P-Δ moments. Herein, stability functions are used for each member to capture these second-order effects in a direct manner.

Geometric imperfections result from unavoidable tolerance during fabrication or erection, and they may be classified as out-of-straightness and out-of-plumbness. These imperfections cause additional moments in column members that result in further degradation of members' bending stiffness. In this paper, geometric imperfections will be considered by either an explicit imperfection modeling, equivalent notional loads, or a further reduction of members' tangent modulus.[4,5]

Material Nonlinearity

Residual stresses result in a gradual axial stiffness degradation. The fibers that have the highest compressive residual stress will yield first under compressive force, followed by the fibers with a lower value of compressive residual stress. Due to this spread of yielding or plasticity, the axial and bending stiffnesses of a column segment is degraded gradually along the length of a member. This stiffness degradation effect will be accounted for later by the tangent modulus concept.[6]

When a wide flange section is subjected to pure bending, the moment-curvature relationship of a section has a smooth transition from elastic to fully plastic. This is because the section yields gradually from extreme fibers which have higher stresses than interior fibers. The gradual yielding effect leads to the concept of a hardening plastic hinge which may be represented simply by a parabolic stiffness reduction function of a plastic hinge.[6] This will be described later.

PRACTICAL CONNECTION MODELING

The connection behavior is represented by its moment-rotation relationship. Extensive experimental works on connections have been performed, and a large body of moment-rotation data has been collected.[7-10] Using these abundant data base, researchers have developed several connection models including: linear; polynomial; B-spline; power; and exponential models. Herein, the three parameter power model proposed by Kishi and Chen[2] is adopted. The Kishi-Chen power model contains three parameters: initial connection stiffness R_{ki}, ultimate connection moment capacity M_u, and shape parameter n. The power model may be written as (Figure 2):

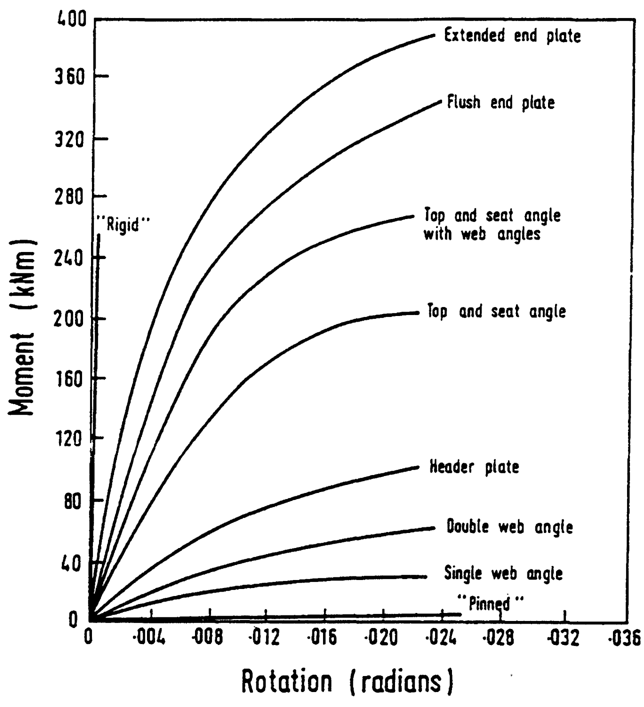

Fig. 1. Schematic moment-rotation curves of various semi-rigid connections.

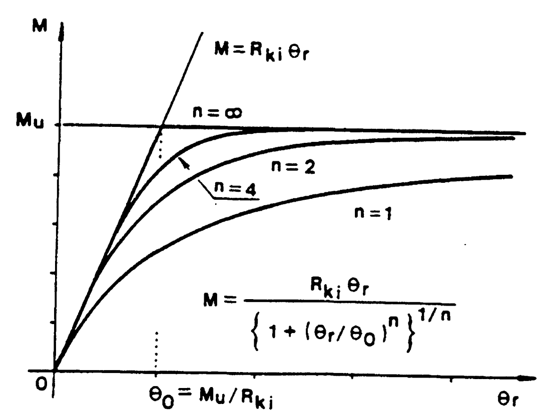

Fig. 2. Moment-rotation behavior of three parameter model.

$$m = \frac{\theta}{(1+\theta^n)^{1/n}} \text{ for } \theta > 0,\ m > 0 \tag{1}$$

where

m = M/M_u
θ = θ_r/θ_o
θ_o = reference plastic rotation, M_u/R_{ki}
M_u = ultimate moment capacity of the connection
R_{ki} = initial connection stiffness
n = shape parameter.

When the connection is loaded, the connection tangent stiffness R_{kt} at an arbitrary rotation θ_r can be derived by simply differentiating Equation 1 as:

$$R_{kt} = \frac{dM}{d\left|\theta_r\right|} = \frac{M_u}{\theta_o(1-\theta^n)^{1+1/n}} \tag{2}$$

When the connection is unloaded, the tangent stiffness is equal to the initial stiffness as:

$$R_{kt} = \frac{dM}{d\left|\theta_r\right|} = \frac{M_u}{\theta_o} = R_{ki} \tag{3}$$

It is observed that a small value of the power index n makes a smooth transition curve from the initial stiffness R_{kt} to the ultimate moment M_u. On the contrary, a large value of the index n makes the transition more abruptly. In the extreme case, when n is infinity, the curve becomes a bilinear line consisting of the initial stiffness R_{ki} and the ultimate moment capacity M_u.

An important task for practical use of the power model is to determine the three parameters for a given connection configuration. Herein, the practical procedures for determining the three parameters are presented for the following four types of connections with angels: single/double web-angle connections; and top and seat angle with/without double web angle connections.

The values of R_{ki} and M_u can be determined by a simple mechanical procedure with an assumed failure mechanism.[2] For single/double web angle connections shown in Figure 3, the initial connection stiffness and the ultimate moment capacity are given by:

$$R_{ki} = G\frac{t_a^3}{3}\frac{\alpha\cosh(\alpha\beta)}{(\alpha\beta)\cosh(\alpha\beta) - \sinh(\alpha\beta)} \tag{4}$$

$$M_u = \frac{2V_{pu} + V_o}{6} d_a^2 \tag{5}$$

where

G = shear moduli
t_a = thickness of web angle
α = 4.2962 when Poisson's ratio is 0.3
β = g_1/d_a
d_a = height of web angle
g_1 = gage distance from the fixed support line to free edge line
V_{pu} = minimum value of V_{py}
V_o = maximum value of V_{py}
V_{py} = plastic shear force per unit length
V_o = shear force capacity per unit length in the absence of bending of web angle.

For the top and seat angle connections shown in Figure 4, the initial connection stiffness and the ultimate moment capacity are given by:

$$R_{ki} = \frac{3EI}{1 + (0.78t_t^2/g_1^2)}\frac{d_1^2}{g_1^3} \tag{6}$$

$$M_u = M_{os} + M_p + V_p d_2 \tag{7}$$

where

EI = bending stiffness of angle's leg adjacent to column face

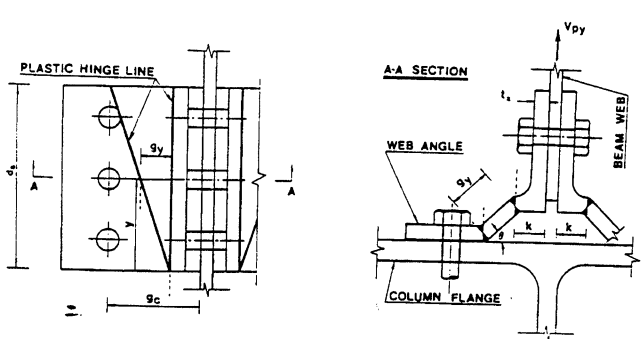

Fig. 3. Mechanism of web angle connection of ultimate condition.

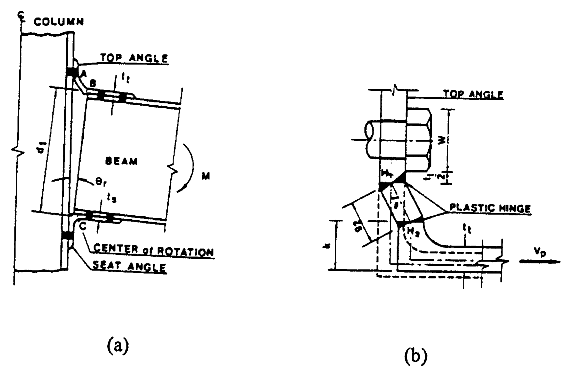

Fig. 4. Top and seat angle connection (a) deflected configuration at elastic condition; and (b) mechanism of top angle at ultimate condition.

Table 1.
Empirical Equations for Shape Parameter *n* (Kishi and Chen 1991)

Connection	*n*	
Single web-angle connection	$0.520\log_{10}\theta_o + 2.291$	for $\log_{10}\theta_o > -3.073$
	0.695	for $\log_{10}\theta_o < -3.073$
Double web-angle connection	$1.322\log_{10}\theta_o + 3.952$	for $\log_{10}\theta_o > -2.582$
	0.573	for $\log_{10}\theta_o < -2.582$
Top and seat angle connection	$2.003\log_{10}\theta_o + 6.070$	for $\log_{10}\theta_o > -2.880$
	0.302	for $\log_{10}\theta_o < -2.880$
Top and seat angle connection with double web angle	$1.398\log_{10}\theta_o + 4.631$	for $\log_{10}\theta_o > -2.721$
	0.827	for $\log_{10}\theta_o < -2.721$

d_1 = distance between centers of legs of top and bottom angles
t_t = thickness of top angle
g_1 $= g_t - D/2 - t_t/2$
D = d_b for rivet fastener
D = W for bolt fastener
g_t = gage distance from top angle's heel to center of fastener holes in leg adjacent to column face
M_{os} = plastic moment capacity at point C
M_p = plastic moment capacity at point H_2 of top angle
V_p = shear force
d_2 $= d + t_s/2 + k$

For top and seat angle connections with double web angles shown in Figure 5, the initial connection stiffness and the ultimate moment capacity are given by:

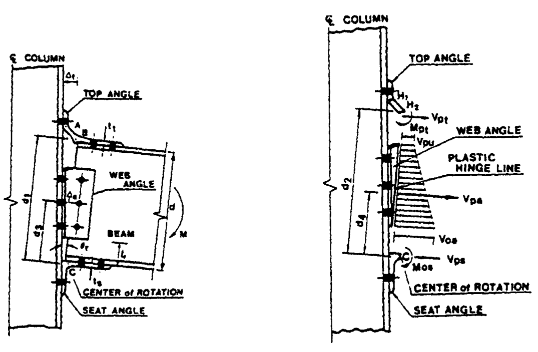

(a) (b)

Fig. 5. Top and seat angle with web angle connection (a) deflected configuration of elastic condition; and (b) applied forces in ultimate state of connection.

$$R_{ki} = \frac{3EI_t d_1^2}{g_1(g_1^2 + 0.78t_t^2)} + \frac{6EI_a d_3^2}{g_3(g_3^2 + 0.78t_a^2)} \tag{8}$$

$$M_u = M_{os} + M_{pt} + V_{pt} d_2 + 2V_{pa} d_4 \tag{9}$$

where

EI_t, EI_a = bending stiffness of legs adjacent to column face of top angle and web angle
g_3 $= g_c - W/2 - t_a/2$
W = diameter of nut
t_a = thickness of top angle
M_{pt} = ultimate moment capacity of top angle
V_{pt} = shearing force acting on plastic hinges
V_{pa} = resulting plastic shear force
d_4 $= \dfrac{(2V_{pu} + V_{oa})}{3(V_{pu} + V_{oa})} d_a + l_l + \dfrac{t_s}{2}$
V_{pu} = shearing force at upper edge of web angle
V_{oa} = shearing force at lower edge of web angle
l_l = distance from bottom edge of web angle to compression flange of beam.

As for the shape parameter *n*, the equations developed by Kishi and Chen et al.[11] are implemented here. Using a statistical technique for *n* values, empirical equations of *n* are determined as a linear function of $\log_{10}\theta_o$ shown in Table 1.

PRACTICAL ADVANCED ANALYSIS

During the past 20 years, research efforts have been devoted to the development and validation of several advanced analysis methods. The advanced analysis methods may be classified into two categories: (1) Plastic-zone method; and (2) Plastic hinge method. Whereas the plastic-zone solution is known as the "exact solution," but can not be used for practical design purposes.[12] This is because the method is too intensive in computation and costly due to its complexity. In recent works by Liew[6] and White,[13] among others, the refined plastic-hinge method has been proposed for two-dimensional frame analysis. The refined plastic-hinge method is developed by a simple modifications of the elastic-plastic hinge analysis to account for the gradual degradation in member's axial and bending stiffness. The refined plastic-hinge method is equivalent to the plastic-zone analysis in its accuracy but is much simpler than the plastic-zone method. Thus, the refined plastic hinge concept is implemented here as a practical method, and its key considerations are discussed in what follows:

Geometric Second-Order Effects

As mentioned previously, stability functions are used to capture the second-order effects since they can account for the effect of the axial force on the bending stiffness reduction of a member. The benefit of using stability functions is that it enables only one element to predict accurately the second-order effect of each framed member.

Stiffness Degradation Associated with Residual Stresses

The tangent modulus concept proposed by Liew[6] is employed here to account for gradual yielding effects due to residual stresses along the length of members under axial loads between two plastic hinges. Herein, the CRC tangent modulus is selected as the better choice between the LRFD E_t and the CRC E_t although the CRC E_t accounts only for the residual stress effect but not geometric imperfection effect.[4] This is because different members with different residual stresses can be incorporated easily in this model, since the effects of geometric imperfections are treated separately from the model. When this model incorporates appropriate geometrical imperfections, it may provide a very good comparison with the plastic-zone solutions.

Stiffness Degradation Associated with Flexure

A gradual stiffness degradation of a plastic hinge is required to represent the distributed plasticity effects associated with bending actions. Herein, we shall introduce the hardening plastic hinge model to represent the gradual transition from elastic stiffness to zero stiffness associated with a fully developed plastic hinge. When the hardening plastic hinges are present at both ends of an element, the incremental force-displacement relationship may be expressed as:[6]

$$\begin{bmatrix} \dot{M}_A \\ \dot{M}_B \\ \dot{P} \end{bmatrix} = \frac{E_t I}{L} \begin{bmatrix} \eta_A\left[S_1 - \frac{S_2^2}{S_1}(1-\eta_B)\right] & \eta_A\eta_B S_2 & 0 \\ \eta_A\eta_B S_2 & \eta_B\left[S_1 - \frac{S_2^2}{S_1}(1-\eta_A)\right] & 0 \\ 0 & 0 & A/I \end{bmatrix} \begin{bmatrix} \dot{\theta}_A \\ \dot{\theta}_B \\ \dot{e} \end{bmatrix} \tag{10}$$

where

$\dot{M}_A$, $\dot{M}_B$, $\dot{P}$ = incremental end moments and axial force, respectively
S_1, S_2 = stability functions
E_t = tangent modulus
I = moment of inertia of cross section
L = length of element
A = area of cross section
η_A, η_B = scalar parameter for gradual inelastic stiffness reduction
$\dot{\theta}_A$, $\dot{\theta}_B$ = incremental rotations at element ends A and B
$\dot{e}$ = incremental axial deformation.

Effect of Semi-Rigid Connection Element

The connection may be modeled as a rotational spring in the moment-rotation relationship represented by Equation 11. Figure 6 shows a beam-column element with semi-rigid connections at both ends. If the effect of connection flexibility is incorporated into the member stiffness, the incremental element force-displacement relationship of Equation 10 is modified as:[6]

$$\begin{bmatrix} \dot{M}_A \\ \dot{M}_B \\ \dot{P} \end{bmatrix} = \frac{E_t I}{L} \begin{bmatrix} S_{ii}^* & S_{ij}^* & 0 \\ S_{ij}^* & S_{jj}^* & 0 \\ 0 & 0 & A/I \end{bmatrix} \begin{bmatrix} \dot{\theta}_A \\ \dot{\theta}_B \\ \dot{e} \end{bmatrix} \tag{11}$$

where

$$S_{ii}^* = \frac{\left(S_{ij} + \frac{E_t I S_{ii} S_{jj}}{L R_{ktB}} - \frac{E_t I S_{ij}^2}{L R_{ktB}}\right)}{R^*} \tag{12a}$$

$$S_{jj}^* = \frac{\left(S_{jj} + \frac{E_t I S_{ii} S_{jj}}{L R_{ktA}} - \frac{E_t I S_{ij}^2}{L R_{ktA}}\right)}{R^*} \tag{12b}$$

$$S_{ij}^* = S_{ij} / R^* \tag{12c}$$

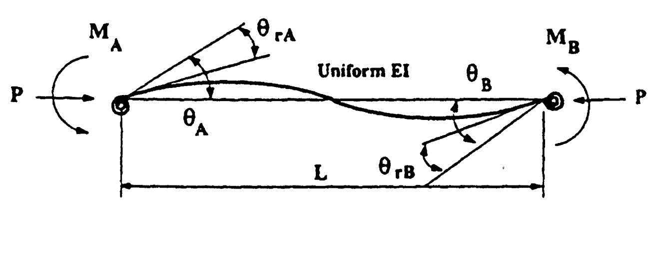

Fig. 6. Beam-column element with semi-rigid connections.

$$R^* = \left(1 + \frac{E_t I S_{ii}}{L R_{ktA}}\right)\left(1 + \frac{E_t I S_{jj}}{L R_{ktB}}\right) - \left(\frac{E_t I}{L}\right)^2 \frac{S_{ij}^2}{R_{ktA} R_{ktB}} \tag{12d}$$

where

R_{ktA}, R_{ktB} = tangent stiffness of connections A and B
S_{ii}, S_{ij} = generalized stability functions
S_{ii}^*, S_{ij}^* = modified stability functions that account for the presence of end connections.

PRACTICAL GEOMETRIC IMPERFECTION MODELING

Geometric imperfection modelings combining with the refined plastic-hinge analysis are discussed in what follows. These include an explicit imperfection modeling method, a notional load method, and a reduced tangent modulus method.

Explicit Imperfection Modeling Method

The AISC Code of Standard Practice[1] limits an erection out-of-plumbness equal to $L_c / 500$ in any story. This imperfection value is conservative in taller frames since the maximum permitted erection tolerance of 50 mm (2 in.) is much less than the accumulated geometric imperfection calculated by $\frac{1}{500}$ times building height. In this study, however, $L_c / 500$ is used for geometric imperfection without any modifications. This is because the system strength is often governed by a weak story which has the out-of-plumbness equal to $L_c / 500$,[14] and the imperfection value may be easily implemented in practical design use.

The frame out-of-plumbness may be used for unbraced frames but not for braced frames. This is because the $P\Delta$ effect caused by out-of-plumbness is diminished by braces in braced frames. As a result, the member out-of-straightness instead of the out-of-plumbness should be used to account for geometric imperfections for braced frames. The AISC Code recommends a maximum fabrication tolerance of $L_c / 1{,}000$ for member out-of-straightness. In this study, the same geometric imperfection of $L_c / 1{,}000$ is adopted by the calibration with the plastic-zone solutions. The out-of-straightness may be reasonably assumed to vary sinusoidally with a maximum in-plane deflection of $L_c / 1{,}000$ at the mid-height. Ideally, many elements are necessary in order to model the sinusoidal out-of-straightness of a beam-column member. In this study, we find that two elements with a maximum deflection at the mid-height of a member are practically adequate to capture the imperfection effects.

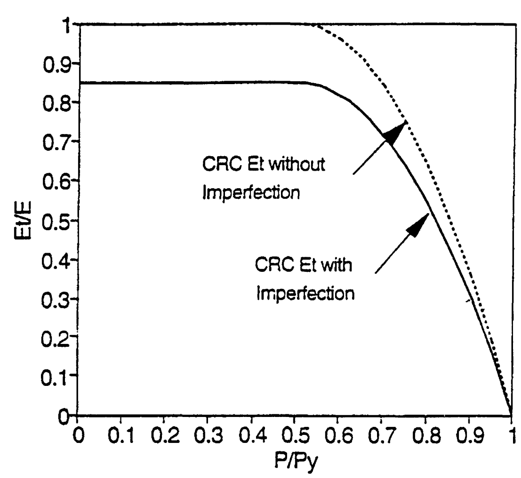

Fig. 7. Further reduced tangent modulus curve.

Equivalent Notional Load Method

The geometric imperfections of a frame may be replaced by equivalent notional lateral loads expressed as a fraction of the gravity loads acting.[15] In this study, the proposed equivalent notional load for practical use is to be $0.002\Sigma P_u$, where ΣP_u is the total gravity load in a story.[5] The notional load should be applied laterally at the top of each story. For braced frames, the notional loads should be applied at mid-height of a column since the ends of the column are braced. In this study, appropriate notional load factor equal to 0.004 is adopted for braced frame. It may be observed this value is equivalent to the geometric imperfection of $L_c / 1{,}000$.

Further Reduced Tangent Modulus Method

The idea of using the reduced tangent modulus method is to further reduce the tangent modulus E_t to account for the geometric imperfections. The degradation of member stiffness due to geometric imperfections may be replaced by an equivalent reduction of member stiffness. This may be achieved by a further reduction factor ϕ_i of tangent modulus as:[4]

$$E_t' = 4 \frac{P}{P_y}\left(1 - \frac{P}{P_y}\right) E\phi_i \text{ for } P > 0.5P_y \tag{13a}$$

$$E_t' = E\phi_i \text{ for } P \le 0.5P_y \tag{13b}$$

where

E_t' = reduced E_t
ϕ_i = reduction factor for geometric imperfection

Figure 7 shows the further reduced tangent modulus curves for the CRC E_t with geometric imperfections. When the tangent modulus E_t is replaced by an appropriate reduced tangent modulus of $0.85E_t$ in CRC column curve, the modified CRC column curve is compared well with the LRFD column curves shown in Figure 8. The same reduction factor of 0.85 may be used for braced frames as well as for unbraced frames. The advantage of this method over the other two methods is its convenience for design use, because it completely eliminates the inconvenience of inputs of the explicit

Table 2. Key Considerations of LRFD and Proposed Methods		
Key Considerations	**LRFD**	**Proposed Methods**
Connection nonlinearity	No procedure	Power model/Rotational spring
Second-order effects	Column curve B_1, B_2 factor	Stability function
Geometric imperfection	Column curve	Explicit imperfection modeling method • $\psi = 1/500$ for unbraced frame • $\delta_c = L_c/1{,}000$ for braced frame Equivalent notional load method • $\alpha = 0.002$ for unbraced frame • $\alpha = 0.004$ for braced frame Further reduced tangent modulus method • $E_t' = 0.85E_t$
Stiffness degradation associated with residual stresses	Column curve	CRC tangent modulus
Stiffness degradation associated wtih flexure	Column curve Interaction equation	Parabolic degradation function

imperfection modeling or the equivalent notional load modeling.

Table 2 summarizes the proposed methods and their key considerations as compared with the LRFD procedures.

VERIFICATION STUDY

In the open literature, no available benchmark problems of semi-rigid frames with geometric imperfections are available for verification study. One way to verify the proposed methods is to make separate verifications for the effects of semi-rigid connections and of geometric imperfections.

Effect of Semi-Rigid Connections

Stelmack[16] studied the experimental response of two flexibly-connected steel frames. A two-story, one-bay frame among his studies is selected as a benchmark frame in the present study. The benchrnark frame was fabricated from the same A36 W5×16 sections, and all column bases are pinned supports in Figure 9. The connections used in the frame were bolted top and seat angle connections of L4×4×½ made of A36 with bolt fasteners of A325 ¾-in. D, and its experimental moment-rotation relationship is shown in Figure 10. Gravity loading of 10.7 kN (2.4 kips) was first applied at third points of the beam of the first floor, and then a lateral load was applied as the second loading sequence. The lateral load-dis-

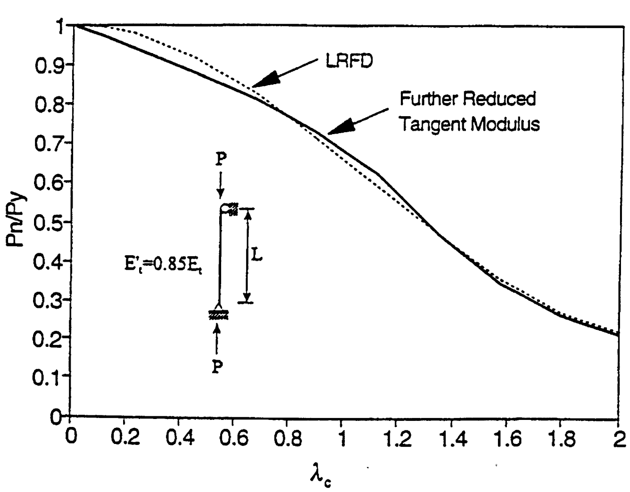

Fig. 8. Comparison of strength curves by further reduced CRC tangent modulus method and LRFD method for axially loaded pin-ended column.

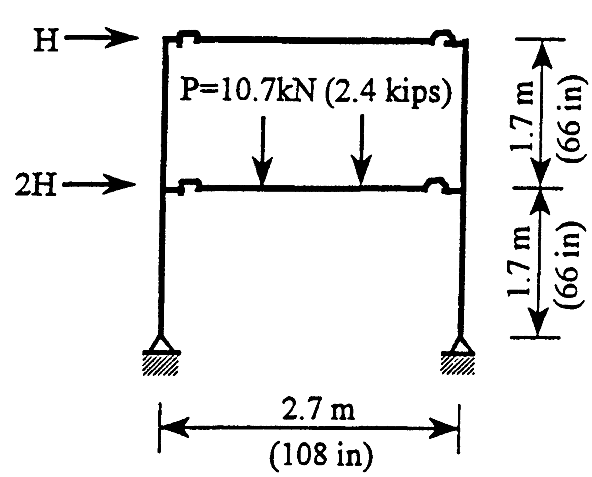

Fig. 9. Configuration of two-story semi-rigid frame for verification study.

placement relationship was provided by the experimental work.

Herein, the three parameters of the power model are determined by a curve fitting with the experimental connection curve as well as by the Kishi-Chen Equations 4-9 and Table 1. The curves by the experiment and by the curve-fitting result in a good agreement as shown in Figure 10. The parameters by Kishi-Chen equations and by the experiment show a difference to some degree as shown in Table 3 and Figure 10. In spite of this difference, Kishi-Chen equations are preferably in practical design since experimental moment-rotation curves are not available in design stages, in general. In the analysis, the gravity load is first applied, followed by the lateral load. The lateral displacements by the proposed methods and by the experiment compare well in Figure 11. As a result, the proposed method is adequate in predicting the behavior and strength of semi-rigid connections.

Effect of Geometric Imperfections

Kim and Chen[4,5] performed a comprehensive verification study of various geometric imperfection effects on frame behavior by comparing the results of the proposed methods with those of the plastic-zone analysis and the conventional LRFD method. Herein, some typical examples are presented in what follows.

The AISC-LRFD column strength curve is used here for a verification of the column strength since it properly accounts for the second-order effect, residual stresses, and geometric imperfections of an isolated column in a practical manner. In the explicit imperfection modeling, the two-element column is assumed to have an initial geometric imperfection equal to $L_c/1{,}000$ at mid-height. In the equivalent notional load method, the notional loads equal to 0.004 times the gravity loads are applied at the mid-height of the column. In the further reduced tangent modulus method, the reduced tangent modulus factor equal to 0.85 is used. The proposed three methods result in a good fit to the LRFD column strengths shown in Figure 12.

Table 3. Comparison of the Three Parameters of Power Model for Verification Study

Method	R_{ki}	M_u	n
Curve-Fitting	4.250 kN-m/rad. (40,000 kip-in/rad.	24.9 kN-m/rad. (220 kip-in./rad.)	0.91
Kishi-Chen	4,499 kN-m/rad. (39,819 kip-in/rad.)	23.5 kN-m/rad. (208 kip-in/rad.)	1.50

Kanchanalai[17] developed exact interaction curves using the plastic-zone analysis for sway frames. In his studies, the members were assumed to have maximum compressive residual stresses of $0.3F_y$ without geometric imperfections. Thus, the curves are adjusted here to account for the effect of geometric imperfections. The AISC-LRFD interaction curves are obtained based on the LeMessurier K-factor approach.[18] The inelastic stiffness reduction factor τ is employed with the LeMessurier procedure for K-factor calculations.[1] Geometric imperfection of $L_c/500$, the notional load factor of 0.002, and the reduced tangent modulus factor of 0.85 are used respectively for the three proposed methods. The proposed methods predict well the strengths of the frame as shown in Figure 13.

ANALYSIS AND DESIGN RULES

Design Format

The proposed methods are based on the LRFD design format. The limit state format may be written as:

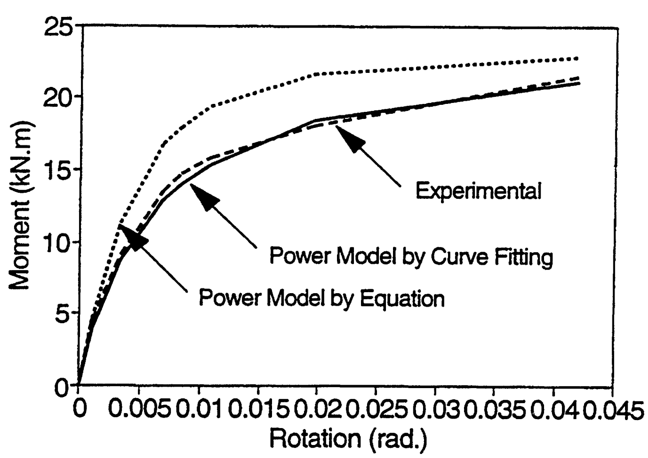

Fig. 10. Comparison of moment-rotation behavior by experiment and three parameter power model for verification study.

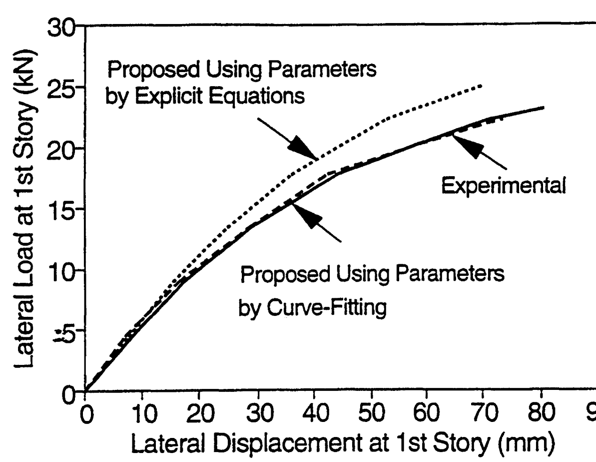

Fig. 11. Comparison of lateral displacements by experiment and proposed methods for verification study.

$$\Sigma\gamma_i Q_i \leq \phi R_n \tag{14}$$

where

γ_i = load factors
Q_i = nominal design loads
ϕ = resistant factors
R_n = nominal resistances.

The limit state format provides a uniform reliability for structures.

Load Combinations

The load combinations in the proposed methods are based on the LRFD load combinations.[1] The member sizes of the structure are determined from an appropriate combination of factored loads.

Live Load Reduction

The live load reduction is based on the ASCE 7-88. It is important to carry out properly the application of the live load reduction in analyzing a structural system. This is because the influence area for each beam and column is generally different and different influence areas result in different reduction factors. In the present study, the live load reduction procedures follow the work of Ziemian and McGuire.[19]

Resistance Factors

Here, as in LRFD, the resistance factors are selected to be 0.85 for axial strength and 0.9 for flexural strength. These resistance factors are included in the computer program for practical design purposes.

Serviceability Limit

The LRFD Specification does not provide specific limiting deflections and lateral drifts. Such limits depend on the function of a structure. Based on the studies by Ad Hoc Committee[20] and Ellingwood,[21] the deflection limits of the girder and the story are adopted as follows:

1) Floor girder live load deflection: L/360
2) Roof girder deflection: L/240
3) Lateral drift: H/400 for wind load
4) Interstory drift: H/300 for wind load

At service load levels, no plastic hinges are allowed to develop since permanent deformations should be prevented under service loads.

Ductility Requirement

Adequate inelastic rotation capacity is required for beam-column members to develop their full plastic moment capacity and to sustain their peak loads The required rotation capacity, i.e., the ductility requirement may be achieved when members are adequately braced and their cross sections are compact. The limitations of the compact section are based on the LRFD Specification. According to the limit on spacing of braces in the LRFD seismic provisions, the L / r_y value should be less than $17{,}200 / F_y$ for beam-columns where F_y is in MPa.

Geometric Imperfection

The magnitude of the geometric imperfections is summarized in Table 2. Users can choose either the explicit imperfection modeling, or the equivalent notional load input, or the further reduced tangent modulus. For simplicity, the further reduced tangent modulus method is recommended.

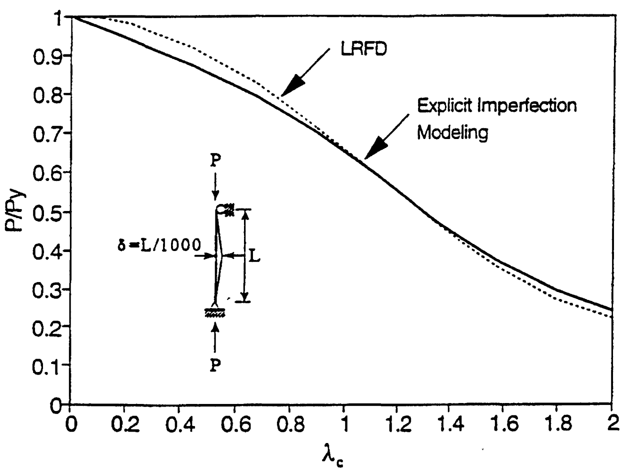

Fig. 12. Comparison of strength curves by explicit imperfection modeling method and LRFD method for axially loaded pin-ended column.

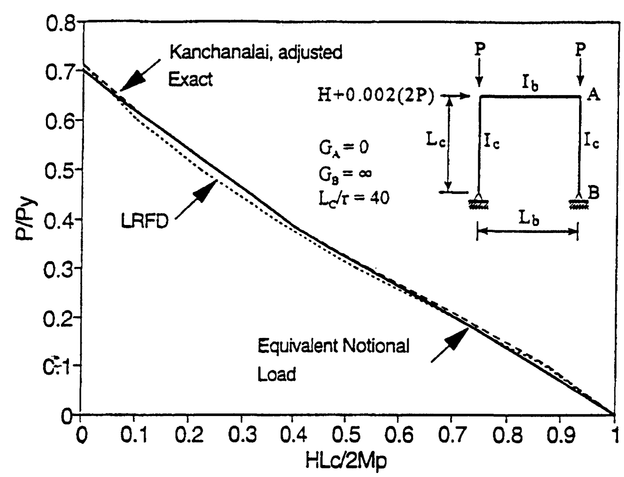

Fig. 13. Comparison of strength curves by equivalent notional load, plastic-zone, and LRFD method for portal frame.

RECOMMENDED ANALYSIS/DESIGN PROCEDURES

The analysis/design of semi-rigid frames is more involved than the analysis and design of rigidly jointed frames. A possible design procedure for semi-rigid frames based on the proposed method is recommended as follows:

Step 1

Preliminary analysis/design assuming rigid frame. The preliminary member sizing is intrinsically dependent on engineer's experiences, the rule of thumb, or some simplified analysis. For example, beam members are usually selected assuming that beams are simply supported and subjected by gravity loads only. For the preliminary sizing of column members, the overall drift requirements should be a good guideline to determine preliminary member sizes rather than the tedious strength checks of the individual column.

Step 2

Preliminary selection of connection type and dimension. The connection types and dimensions should be determined by considering the overall flexibility of a structural system since the connection flexibility influences the second-order moment of a structural system. For illustration, relatively flexible connections such as single/double web angles may be used for a braced system, and conversely, relatively rigid connections suchs as extended header plates may be used for an unbraced system. The dimensions of connections may be-selected from the resulting member forces and displacements information in Step 1.

Step 3

Determination of connection parameters. The power model for connections contains three parameters and they can be determined by Equations 4–9 and Table 1 for the connection types and dimensions determined in Step 2.

Step 4

Analysis of semi-rigid structural system. Once the preliminary member and connection sizes are determined in Steps 1–3, the refined plastic hinge analysis may be performed to consider the effect of semi-rigid connections and geometric imperfections.

Step 5

Check for strength, serviceability, and ductility. The adequacy of system and its component member strength can be directly evaluated by comparing the predicted ultimate loads with the applied factored loads. The serviceability of a structural system should be also checked to ensure the adequacy of the system and member stiffness at service loads. Adequate ductility is required for members in order to develop their full plastic moment capacity. The required ductility may be achieved when members are adequately braced and their cross sections are compact.

Step 6

Local strength checks of members and connections. Since the proposed analysis account for only the global behavior effects, the independent local strength checks of members and connections are required based on the LRFD Specification.

Step 7

Adjustment of member and connection sizes. If the conditions of Steps 6–7 are not satisfied, appropriate adjustments of member and connection sizes should be made. The system

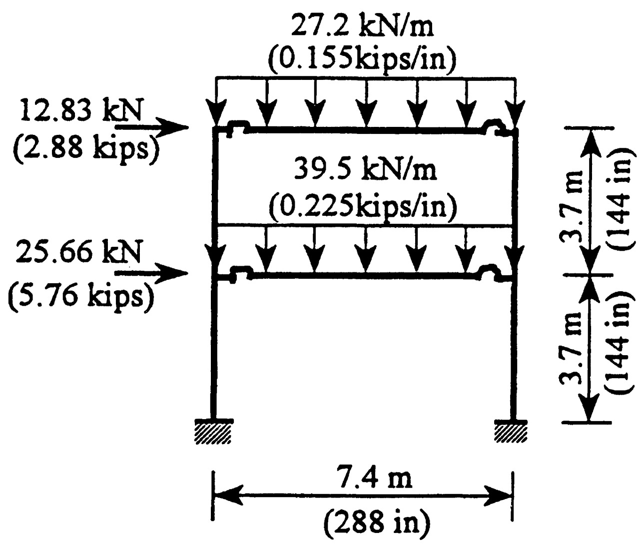

Fig. 14. Configuration of two-story semi-rigid frame for design example.

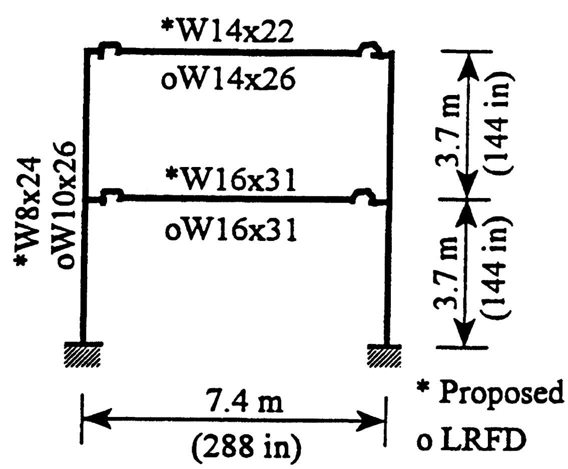

Fig. 15. Comparison of member sizes by proposed methods and LRFD method for design example.

behavior is influenced by the combined effects of members and connections. As an illustration, if an excessive lateral drift occurs in a structural system, the drift may be reduced by increasing member size or by using more rigid connections. If the strength of a beam exceeds the required strength, it may be adjusted by reducing the beam size or using more flexible connections. Once the member and connection sizes are adjusted, iteration of Steps 2–7 leads to an optimum design.

DESIGN EXAMPLE

Barakat[22] studied several frames with semi-rigid connections. In this study, the two-story, one-bay semi-rigid frame is selected for the present case study. Herein, the design of this semi-rigid frame follows the analysis and design rules and procedures described above. The member sizes determined by the proposed methods are compared with those determined by the modified LRFD method proposed by Barakat.[22]

Description of Frame

The height of each story is 3.7 m (12 ft) and the width is 7.4 m (24 ft). The frame was subjected to vertical distributed loads and concentrated lateral loads according to the load combination of $1.2D + 1.3W + 0.5L$ shown in Figure 14. All connections are top and seat angle of L6×4.0×½×8.0 with double web angles of L4×3.5×¼×8.5 made of A36 steel with bolt fasteners of A325 ⅞-in. D.

Analyses

The yield stress was selected as 250MPa (36 ksi), and Young's modulus was 200,000MPa (29,000 ksi). The analyses were carried out by the proposed three methods. The explicit geometric imperfection was assumed to be $\psi = 2/1{,}000$, the equivalent notional load was equal to $0.002\Sigma P_u$, and the further reduced tangent modulus was adopted as $0.85E_t$. The connection parameters of the power model was calculated as the initial connection stiffness R_{ki} of 40,021 kN-m/rad. (354,232 kip-in/rad.), the ultimate moment capacity M_u of 128 kN-m (1,131 kip-in.) and the shape parameter n of 1.14 by using Equations 4-9 and Table 1. The vertical and lateral loads were applied to the frame at the same time in an incremental manner. The resulting ultimate loads were compared with the factored applied loads, and member sizes were adjusted.

Member Size

All three methods result in identical member sizes. They are compared in Figure 15 with those determined by the modified LRFD method proposed by Barakat and Chen.[22-24] The sizes of member sections are chosen such that the width of the beam flange is less than that of the column flange. This is due to the need of detailing of beam-to-column semi-rigid connections. The member sizes by the proposed methods are generally one size smaller than those by the modified LRFD method, because the proposed methods possess the benefit of inelastic moment redistribution that leads to a reduced steel weight for highly indeterminate steel structures.

Serviceability

The overall drift of the first-order analysis under wind load is calculated as $H/218$ which does not meet the drift limit of $H/400$. When the column sizes are increased from W8×24 to W12×26. the overall drift limit is found to be $H/408$ which satisfies the drift limit. The deflections in the beams under live load are smaller than the limit of $L/360$.

SUMMARY AND CONCLUSIONS

Three practical methods are developed for semi-rigid frame design using the refined plastic hinge analysis. They are the explicit imperfection modeling method, the notional load method, and the reduced tangent modulus method. The practical procedures for determining connection parameters are provided for a given connection configuration. The proposed methods can predict accurately the combined effects of connection, geometric, and material nonlinearities for semi-rigid frames. The strengths predicted by these methods are compared well with those available experiments. The proposed methods provide a practical procedure for the LRFD design of semi-rigid frames. To this end, the analysis/design rules and procedures for practical design of semi-rigid frames are described in details. The methods do not require separate member capacity checks including the calculations of K-factor. Since the proposed methods strike a balance between the requirement for realistic representation of actual behavior and failure mode of a structural system and the requirement for simplicity in use, it is considered that in both these respects, all three methods are satisfactory, but the further reduced tangent modulus method appears to be the simplest and is therefore recommended for general use.

REFERENCES

1. American Institute of Steel Construction, *Manual of Steel Construction, Load and Resistance Factor Design*, 2nd Ed., Vol. 1 and 2, Chicago, IL, 1993.
2. Kish, N. and Chen, W. F., "Moment-rotation Relations of Semi-rigid Connections with Angles," ASCE *Journal of Structural Engineering*, 116, 7, 1990, pp. 1813–1834.
3. Chen, W. F. and Lui, E. M., *Stability Design of Steel Frames*, CRC Press, 1991, 380 pp.
4. Kim, S. E. and Chen, W. F., "Practical Advanced Analysis for Braced Steel Frame Design," *Structural Engineering Report No. CE-STR-95-11*, School of Civil Engineering, Purdue University, West Lafayette, IN, 1995, 36 pp.
5. Kim, S. E. and Chen, W. F., "Practical Advanced Analysis for Unbraced Steel Frame Design," *Structural Engineering Report No. CE-STR-95-15*, School of Civil Engineering, Purdue University, West Lafayette, IN, 1995, 36 pp.
6. Liew, J. Y. R., "Advanced Analysis for Frame Design,"

Ph.D. Thesis, School of Civil Engineering, Purdue University, West Lafayette, IN, 1992, 392 pp.

7. Goverdhan, A. V., "A Collection of Experimental Moment-rotation Curves and Evaluation of Prediction Equations for Semi-rigid Connections," *Master's Thesis*, Vanderbilt University, Nashville, TN, 1983, 490 pp.
8. Nethercot, D. A., "Steel Beam-to-column Connections—a Review of Test Data and its Applicability to the Evaluation of Joint Behavior in the Performance of Steel Frames," *CIRIA Project Record, RP 338*, 1985.
9. Kishi, N. and Chen, W. F., "Data Base of Steel Beam-to-column Connections," *Structural Engineering Report No. CE-STR-86-26*, School of Civil Engineering, Purdue University, West Lafayette, IN, 1986, 653 pp.
10. Chen, W. F. and Kishi, N., "Semi-rigid Steel Beam-to-column Connections: Data Base And Modeling," ASCE *Journal of Structural Engineering*, 115, 1, 1989, pp. 105–119.
11. Kishi, N., Chen, W. F., Goto, Y., and Matsuoka K. G., "Applicability of Three-Parameter Power Model to Structural Analysis of Flexibly Jointed Frames," *Proc. Mechanics Computing in 1990's and Beyond*, Columbus, OH, May 20–22, 1991, pp. 233–237.
12. Chen, W. F. and Toma, S. Editors, *Advanced Analysis of Steel Frames*, CRC Press, 1994, 383 pp.
13. White, D. W., "Plastic Hinge Methods for Advanced Analysis of Steel Frames," *Journal of Constructional Steel Research*, Vol. 24, No. 2, 1993, pp. 121–152.
14. Maleck, A. E., White, D. W., and Chen, W. F., "Practical Application of Advanced Analysis in Steel Design," *Presented at the 4th Pacific Structural Steel Conference*, Singapore, October 1995.
15. Liew, J. Y. R., White, D. W., and Chen, W. F., "Notional-load Plastic-hinge Method For Frame Design," ASCE *Journal of Structural Engineering*, 120(5), 1994, pp. 1434–1454.
16. Stelmack T. W., "Analytical and Experimental Response of Flexibly-connected Steel Frames," *M.S. Thesis*, Department of Civil, Environmental, and Architectural Engineering, University of Colorado, 1982, 134 pp.
17. Kanchanalai, T., "The Design and Behavior of Beam-columns in Unbraced Steel Frames," *Aisi Project No. 189, Report No. 2*, Civil Engineering/structures Research Lab., University of Texas, Austin, TX, 1977, 300 pp.
18. Lemessurier. W. J., "A Practical Method of Second Order Analysis, Part 2—Rigid Frames," AISC *Engineering Journal*, 2nd Qtr., Vol. 14, 1977, pp. 49–67.
19. Ziemian, R. D. and Mcguire, W., "A Method for Incorporating Live Load Reduction Provisions in Frame Analysis," AISC *Engineering Journal*, 1st Qtr., Vol. 29, 1992, pp. 1–3.
20. An Hoc Committee on Serviceability, "Structural Serviceability: a Critical Appraisal and Research Needs," ASCE *Journal of Structural Engineering*, 112(12), 1986, pp. 2646–2664.
21. Ellingwood, "Serviceabilitv Guidelines for Steel Structures," AISC *Engineering Journal*, 1st Qtr., Vol. 26, 1989, pp. 1–8.
22. Barakat, M., "Simplified Design Analysis of Frames with Semi-rigid Connections," *Ph.D. Dissertation*, School of Civil Engineering, Purdue University, West Lafayette, In, 1989, 211 pp.
23. Barakat, M. and Chen, W. F., "Practical Analysis of Semi-rigid Frames," AISC *Engineering Journal*, 2nd Qtr., Vol. 27, 1990, pp. 54–68.
24. Barakat, M. and Chen, W. F., "Design Analysis of Semi-rigid Frames, Evaluation and Implementation," AISC *Engineering Journal*, 2nd Qtr., Vol. 28, 1991, pp. 55–64.

LIST OF SYMBOLS

E	modulus of elasticity
E_t	tangent modulus
E_t'	further reduced E_t
F_y	material yield stress
G	shear moduli
G_A, G_B	ratio of bending stiffness of columns versus that of beams at beam-to-column joint, subscripts apply to respective ends of column
I_b, I_c	moment of inertia of cross section, subscripts b and c denote beam and column
L	column length
L_b, L_c	length, subscripts b and c denote beam and column
m	Nondimensional connection moment, M/M_p
M_p	plastic moment capacity
M_u	ultimate moment capacity of connection
$\dot{M}_A$, $\dot{M}_B$, $\dot{P}$	incremental end moments and axial force
P, M	second-order axial force and bending moment
n	shape parameter
P_y	squash load
Q_i	nominal design loads
R_{ki}	Initial connection stiffness
R_{kt}	tangent stiffness of connections
R_{ktA}, R_{ktB}	tangent stiffness of connections A and B
R_n	nominal resistances
S_1, S_2	stability functions
S_{ii}, S_{ij}	generalized stability functions
S_{ii}^*, S_{ij}^*, S_{jj}^*	modified stability functions that account for the presence of end connection
α	equivalent notional load factor in Table 2
γ_i	load factor
δ_c	geometric imperfection at mid-height of column in Table 2
η_A, η_B	scalar parameter for gradual inelastic stiffness reduction
θ	ratio of arbitrary rotation to reference plastic rotation of connection

θ_o	reference plastic rotation of connection, M_u / R_{ki}
θ_r	arbitrary rotation of connection
$\dot{\theta}_A$, $\dot{\theta}_B$	incremental rotations at element ends A and B
λ_c	column slenderness parameter
ϕ	resistant factor
ϕ_i	reduction factor for geometric imperfection
ψ	out-of-plumbness